Journal of Materials Chemistry C

Accepted Manuscript

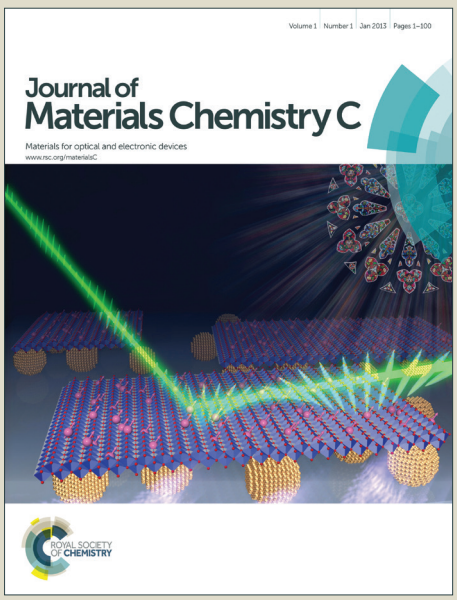

ROYAL SOCIETY OF CHEMISTRY

www.rsc.org/materialsC

Journal Materials Chemistry C

ARTICLE

Transparent composites prepared by bacterial cellulose and castor oil based polyurethane as substrate for flexible OLEDs

Received 00th January 20xx,
Accepted 00th January 20xx

DOI: 10.1039/x0xx00000x

www.rsc.org/

E. R. P. Pinto,[a‡] H. S. Barud,[a,b‡*] R. R. Silva,[a] M. Palmieri,[a] W. L. Polito,[c] V. L. Calil,[c] M. Cremona,[d] S. J. L. Ribeiro,[a] and Y. Messaddeq[a]

Flexible and transparent composites were prepared from bacterial cellulose (BC) and castor oil based polyurethane (PU), The new BC/PU composites exhibit excellent transparency (up to 90 %) in the visible region and great mechanical properties, with tensile strength up to 69 MPa and Young's Modulus up to 6 GPa. The resulting free-standing thin films achieved low surface roughness (below 1 nm), whose properties suggest a potential candidate substrate for flexible light emitting devices. Nevertheless, the fabrication of Flexible Organic Light Emitting Diode (flexible OLED) were successfully investigated by using flexible transparent BC/PU membranes rather than standard flat glass substrates.

Introduction

Bacterial cellulose (BC) membranes are produced by some bacteria such as the specie *Gluconacetobacter xylinus*.[1] Essentially, BC is a hydrogel formed by 1 wt% of an interesting 3D network of fibers with diameters below 100 nm (nanoscale range). Unlike plant-based cellulose fibers, the BC nanofibers have many unique properties including high degree of polymerization and crystallinity besides higher tensile strength (200 - 300 MPa) and Young's modulus (up to 78 GPa) which make them 8 times stronger than stainless steel.[2] These particular features introduces the BC membranes into a wealth of applications since reinforcing agent for composites throughout substrates to highly desired optical materials.[3] In fact, BC nanofibers are very strong but also very lightweight. Because the small lateral dimensions of individual BC nanofibers, they display negligible light scattering whose particularly rich and exciting physics comes into play as an attractive material for reinforcement of transparent substrates for electronic displays.

At the present, organic light emitting diode (OLED) have been traditionally fabricated on rigid glass sheet substrates.[4] However, flexible polymer substrates have been expected as potential alternative in replacing the glass substrate.[5-7] An additional and highly desirable feature is addressed to the use of high content of biopolymers in the manufacturing of flexible substrates. Owing to their inherent nature, the BC nanofibers possess high tensile strength, a low coefficient of thermal expansion (i.e. 0.1 ppm.K^{-1})[8] besides an exceptional flexibility which introduce significant improvements on the mechanical properties of derived composites.

Many works have been focused on the pursuit for rational design of BC composite materials with relevant optical and mechanical properties and commercially comparable to the current engineered plastics.[5, 7, 9] An increasing number of approaches have been compelled to the fabrication of transparent nanobiocomposites based on BC and renewable biopolymers sources. Some of these nanobiocomposites include BC/chitosan,[10] BC/polyhydroxybutirate,[11] BC/polyvinyl alcohol,[12] BC/boehmite-epoxi-siloxane,[13] BC/poly(L-lactic acid),[14] among others. Nevertheless, several works also have been dedicated in the fabrication of highly transparent BC composites based on the impregnation with resins. Yano et al.[15] developed highly transparent composites based on BC membranes impregnated with epoxy, acrylic and phenol-formaldehyde resins. In general, the composites display a high fiber content (70 wt%) with outstanding mechanical strength and low thermal expansion coefficient.[15]

Among various resins from renewable resources,[16] polyurethane (PU) is a versatile polymer produced from different raw materials and widely used in several applications such as hard and flexible foams, thermoplastics, thermosetting, coatings, elastomers and adhesives. The main advantage of the use of PU resins is their segmented domain structure, which can be tailored over a considerable range through the selection of the raw materials, their relative proportions, and the processing conditions. Vegetable oils such as canola oil, corn oil, linseed oil, palm oil, soybean oil and sunflower oil have been explored as raw source to the manufacture of PU resins.[17] Noteworthy, castor oil is one the most investigated natural oil polyol to prepare PU. The castor

[a] *Institute of Chemistry - São Paulo State University - UNESP, Araraquara, São Paulo 14801-970, Brazil.*
[b] *Centro universitário de Araraquara - UNIARA, Araraquara, São Paulo 14801-320, Brazil.*
[c] *Institute of Chemistry - São Paulo University - USP, São Carlos, São Paulo 13560-250, Brazil*
[d] *Department of Physics - Pontifical Catholic University - PUC, Rio de Janeiro 22451-900, Brazil*
*Corresponding author: hernane.barud@gmail.com

oil is composed majority (i.e. 90%) by tri-ester of rincinoleic acid and glycerin, which deals to an interesting precursor rich in groups such as hydroxyl groups and carbon-carbon double bond.[18-20]

The PU resin can be synthesized as a chemically active prepolymer. Essentially, the PU prepolymer has free-isocyanate groups, which in turn easily bind with hydroxyl groups to produce urethane bonds. In this sense, it is feasible and even predictable that PU prepolymer may have the ability to fashion a strong interface with hydroxyl groups present onto the surface of BC nanofibers through of urethane bonds. Indeed, several works have investigated the use of plant cellulose[22-25] or lignin[21] and PU resin to produce improved composites. To date, Manuspiya et al.[26, 27] have exploited the design of films composites based on impregnation of commercial PU resin into dried BC membranes (10 - 50 %) for flexible OLEDs. The BC-derived films were found to achieve a reduced water absorption after the impregnation of PU besides remarkable flexibility and transparency (> 80 % at 550 nm).[27] It should be pointing out that the most of the works relies on PU derived from petrochemical resources.[28, 29]

Herein, transparent and bendable nanocomposites with high bio-content were prepared by the impregnation of PU prepolymer derived from castor oil into dried BC membranes. The BC/PU composites displayed high BC fiber content (up to 70 %), low roughness, high thermal stability, and excellent mechanical properties. Flexible OLEDs based on BC/PU membranes were fashioned and their electric and optical properties were evaluated.

Experimental

Materials

Refined Castor Oil First Special Grade (FSG) was produced from a local oil company, Aboissa. Trimethylolpropane, propylene glycol, xylene, ethyl glycol acetate and ethanol puriss. p.a. were all purchased from Sigma Aldrich. Toluene-diisocyanate 80/20 (TDI) was purchased from Brazmo. 2-phenylpyridine)iridium(III) ($Ir(ppy)_3$), Copper phthalocyanine (CuPc, 99%), N,N'-bis(1-naphtyl)-N,N'-diphenyl-1,1'-biphenyl-4,4'-diamine (NPB), 4,4'-bis(carbazol-9-yl)biphenyl (CBP), 2,9-dimethyl-4,7-diphenyl-1,10-phenanthroline (BCP), tris(8-hydroxyquinoline) aluminum (Alq_3) and aluminum (Al) were all purchased from LumTec Corp. SiO_2 and Ceramic In_2O_3:SnO_2 (90:10 wt%, 99.99 % purity) targets were purchased from Kurt J. Lesker.

Culture Media for the production of membranes of bacterial cellulose

Never-dried BC membranes (5 x 6 cm, 5 mm thick) were produced from an isolated culture of a wild strain of *Gluconacetobacter xylinus* (American Type Culture Collection, ATCC 23769). Cultivation medium was conducted at 28 °C for 96 h in trays with dimensions of 30 cm x 50 cm, containing sterile medium composed of glucose 50 $g.L^{-1}$, yeast extracts 4 $g.L^{-1}$, anhydrous disodium phosphate 2 $g.L^{-1}$, heptahydrated magnesium sulphate 0.8 $g.L^{-1}$, ethanol 20 $g.L^{-1}$. After 96 h, hydrated BC hydrogels membranes were about 3 mm thick. BC membranes were composed of 1 wt% cellulose and 99 wt% water. Membranes were washed several times under water flux. An aqueous solution of NaOH 1 wt% at 70 ºC was added in order to remove remaining bacteria and water until achieve a neutral pH. Dried BC membranes were obtained by drying hydrated membranes at 80 °C between two Teflon plates.

Syntheses of castor oil based polyurethane prepolymer

The polyurethane prepolymer (PU) was synthesized with TDI and a polyol consisting of castor oil as main component. The synthesis of PU prepolymer was performed in a stainless steel reactor (1 Kg of capacity) at ambient pressure (1 atm). The molar ratio between isocyanate and hydroxyl groups was set to 1.1-1.0 and the prepolymer had 4% of free-isocyanate. The synthesis of PU prepolymer was reported by De Carlo (2002),[30] which used the following components: castor oil (OH = 180 $mgKOH.g^{-1}$ sample), trimethylolpropane, propylene(glycol), TDI, xylene and ethyl glycol acetate. The polymerization reaction was placed in a reactor where the components were added at one shot. The reaction was conducted for 8 h at 85 °C under nitrogen atmosphere and vigorous agitation.

Preparation of flexible transparent BC/PU composites

Dried BC membranes (5 cm x 6 cm, 20 µm thick) were coated with neat PU prepolymer (4 wt% isocyanate-free) on both sides. The membrane was held by a handy rectangular Teflon device with screws at the corners. Therefore, BC membrane was merged in solvents of different polarity, which in turn were selected according to low cost of processability and afforded the best interface with PU prepolymer (i.e. prevention of phase separation). a) The first solvent was ethanol in order to remove any residual water in the surface of BC nanofibers. Afterwards, ethanol was exchanged by merging the BC membrane in ethyl glycol acetate, a common solvent of PU prepolymer. Two periods of time were chosen for this study: 72 h and 120 h. The samples were named as BC/PU72 and BC/PU120 b) BC membranes were coated with neat PU prepolymer (4 wt% of free-isocyanate) for approximately 5 minutes. c) BC/PU composites were dried at ambient temperature for 24 h in a rectangular Teflon device.

Preparation of flexible transparent BC/PU membrane substrate for flexible OLED

The BC/PU composite were coated with SiO_2 and indium tin oxide (ITO) thin films seeking increase the electrical conductance of the membrane. The depositions were carried out in Åmod Series Coating Systems from Angstrom Engineering, equipped with a 3-inch magnetron gun. The radio frequency power of 13.56 MHz was supplied by an radio frequency generator matched to the target by a tuning network, both from Advanced Energy. SiO_2 and ITO were deposited using 100 W and 80 W power deposition for final

thickness of 100 nm and 300 nm, respectively. The work pressure of 0.27 Pa was applied for both materials.

Flexible OLED devices were fabricated by high vacuum thermal evaporation of the organic materials with the usual $Ir(ppy)_3$ based OLED architecture: CuPc, NPB, co-deposited layer of CBP as matrix and $Ir(ppy)_3$ as dopant, BCP, Alq_3 and Al. The base pressure was 1.0 mPa (~8×10^{-6} Torr) and during evaporation the pressure was between 1.3 mPa and 6.7 mPa. The deposition rates for organic and Al films were 3 and 18 $nm.min^{-1}$, respectively. In order to compare the flexible OLED performance, a reference device was fabricated using a flat glass slide as substrate.

Optical and structural properties of BC/PU composites

The transmission spectra were recorded in an ultraviolet-visible-near infrared, Varian – CARY 500 Spectrophotometer in the 800 - 300 nm wavelength interval. Refractive index was obtained by using a Metricon mod. 2010 prism coupler equipped with a He–Ne laser operating at 543.5nm. Scanning electron microscopy (SEM) measurements were performed with a SEM-JEOL 6700F. Samples were covered with a 3 nm tick Pt layer. AFM was performed with an Agilent 5500 SPM AC Mode III (Agilent Technologies in ambient conditions (22 °C, 45 – 55 % relative humidity) over areas of 5 μm x 5 μm and 1 μm x 1 μm. The instrument was equipped with silicon (aluminum coating) tip with resonance frequency 204 – 497 KHz and force constant 10 – 130 $N.m^{-1}$, operated in tapping mode. The measurements were repeated five times for comparable topological analysis. Image and roughness analysis were conducted using Gwyddion 2.31 software.

X-ray diffraction patterns were obtained with a Siemens Kristalloflex diffractometer using nickel filtered Cu Kα radiation, step pass of 0.02° and a step time of 3 s, from 5° to 50° (2θ angle). The mechanical measurements were performed at room temperature with a Dynamic Mechanical Analyzer (DMA) 2980 from TA Instruments, equipped with a film tension clamp. Specimens' dimensions were 1 cm x 0.25 cm. Thickness values varied from 10 μm to 35 μm. A preload force of 0.01 N was used and the force ramp 18 $N.m^{-1}$ until the rupture of sample. The device was previous calibrated and 10 measurements for each sample were achieved to ensure the reproducibility of the results.

Characterization of the BC/PU composite as substrate for flexible OLED

The electrical properties of the functionalized BC/PU composite and glass substrate were measured using four-point probe technique, in an ECOPIA Hall Effect Measurement System HS 3000. The film thickness was measured using a Dektak6M Stylus Profile from Veeco. The luminance was measured directly by a calibrated Konica Minolta Luminance Meter LS-100. The current–voltage (I–V) characteristics were measured with a programmable voltage current source (Keithley 2400).

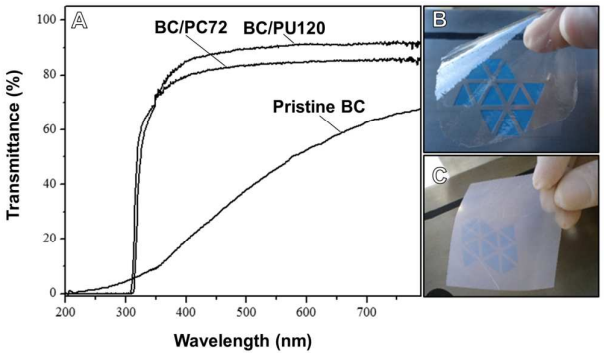

Figure 1. (A) Transmittance spectra in the ultraviolet-visible wavelength interval (200 – 800 nm) for pristine dried BC membrane and BC/PU composite resulted from solvent exchange process within 72 h and 120 h. The digital images in (B) and (C) highlights the difference of transparency between BC/PU composite resulted from solvent exchange process within 72 h and dried BC membrane, respectively.

Results and discussion

The nominal composition and thickness of resulting flexible and freestanding BC/PU composites are described in the Table 1. Pristine dried BC membranes showed usual poor transparency while BC/PU composites, possessing a high content of cellulose (>70 wt%), exhibited high transparency. Additionally, the BC/PU nanocomposite displayed reliable flexibility and macroscopic homogeneity as highlighted in the pictures of Figure 1a. The transmittance spectra in the ultraviolet-visible region of pristine dried BC membranes and BC/PU composites dried in different period of times are shown in Figure 1a. The blue vector picture behind the bended BC/PU composite was clearly visible in Figure 1b rather than translucent pristine BC membrane shown in Figure 1c. The transmission spectra of the BC/PU composites were carefully evaluated taking into account the eventual disparities of the sheet thickness among the samples.

As expected, pristine BC membrane displayed very poor transparency in the UV-vis region with transmittance values of 8 % at 350 nm and 63 % at 700 nm. On the other hand, BC/PU composites show a significantly increase on transparency with transmittance larger than. 70 % at 350 nm. The BC/PU composites showed high transparency in the visible range. For example, BC membranes subjected to 72 h of solvent exchange, BC/PU72 displayed a transparency of 82 % at 700 nm whereas BC membranes that were allowed to exchange solvent for additional 48 h (120 h in total, BC/PU120), exhibited a transparency of 90 % at 700 nm. A slight decrease on the transparency was found for BC/PU72 once it comprised a composite with more BC nanofibers content, which in turn

Table 1. Specifications of the composition of the BC/PU composites

	BC (wt%)	PU prepolymer (wt%)	Thickness (μm)
Pristine BC	100	—	20
BC/PU72	79	21	21
BC/PU120	74	26	22
Pure PU film	—	100	15

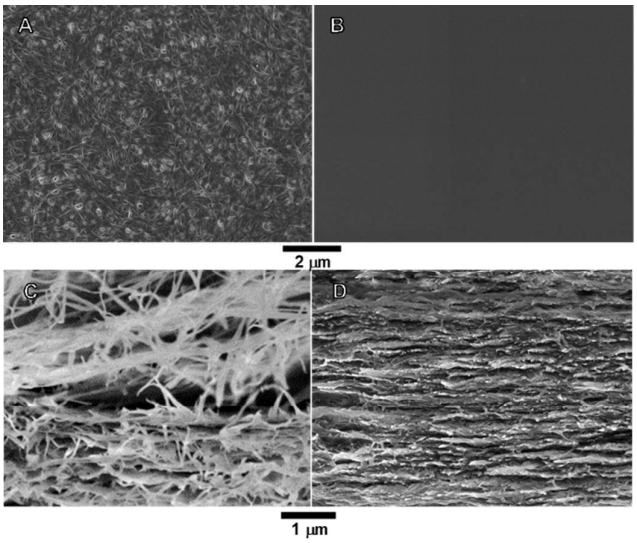

Figure 2. SEM images of (A) the surface of pristine dried BC membrane and (B) surface of BC/PU composite resulted from solvent exchange process within 72 h. (C) Cross-section of pristine dried BC membrane and (D) cross-section of BC/PU composite resulted from solvent exchange process within 72 h.

addresses additional light scattering.

The notorious transparency of BC/PU composites conceives the overlapping of the optical properties of both pure PU films and the 3D network assembly of BC nanofibers. It should be noted that the refractive index (η) is the most striking feature which has to be taken in consideration on the design of composites with enhanced optical quality. Essentially, BC membrane presents two η values: 1.618 for the parallel direction toward the crystal axis ($\eta_{//}$) and 1.544 for the perpendicular direction toward the chain orientation ($\eta_{\_|\_}$).[31] In fact, the contrast between the refractive index of the cellulose fibers (η > 1.5) and air (η = 1), existing in the interstices of dried pristine BC membrane, causes light scattering. However, the BC membrane became very transparent after the introduction of PU prepolymer. We carried out the measurement of the η value of the pure PU film derived from castor oil and BC/PU composites through the M-lines technique. In fact, all BC/PU composites exhibited the same η value of 1.544 whereas the pure PU film had a value of 1.526. Therefore, it is suggested that the proximity between the η value of the pure PU film and the $\eta_{\_|\_}$ value of the BC nanofibers may elucidate the remarkable transparency of the BC membranes coated with a PU resin.

Figure 2, a and b, show the SEM images of the surface of pristine dried BC and BC/PU72 composite, respectively. The surface of a dried BC membrane was formed by a compact 3D network of random assemblages of BC nanofibrils bundles that clutch into flat ribbon- and filamentary-shaped cellulose fibers with diameter ranging from 50 to 100 nm.[9, 15, 32] Figure 2b shows the BC membrane surface when it was totally covered by PU resin. The 3D network of cellulose nanofibers completely disappeared on the surface of BC/PU composites after the impregnation with PU. The cross section image for BC shown in Figure 2c, reveals unoriented BC nanofibrils organized into plate-like structures loosely spaced each other. It is worth to pointing up that any change of morphology of BC

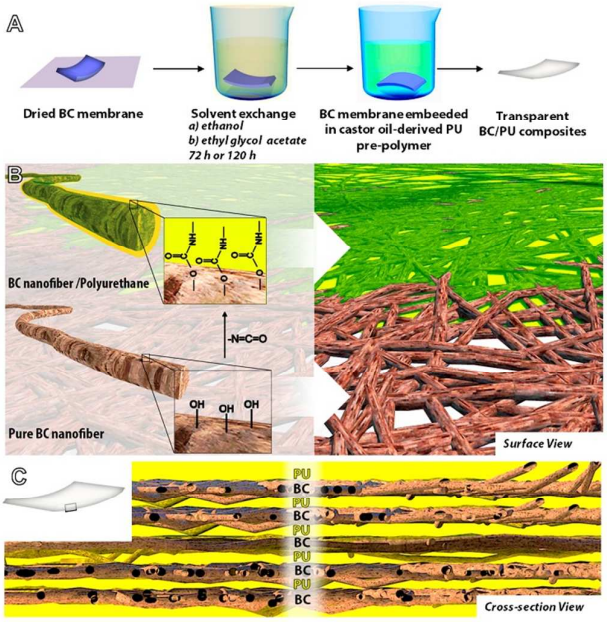

Figure 3. Schematic illustration of the (A) protocol for the fabrication of BC/PU composites via solvent exchange process (B) surface view of the interface of BC nanofibers naturally rich in hydroxyl bonds and the post-modification with PU prepolymer by the formation of urethane bonds. (C) Cross-section view of the BC/PU composite suggested the formation of alternated layers of BC nanofibers filled with PU.

nanofibers was observed in the nanocomposites. On the other hand, the SEM image of the cross section of BC/PU72 composite in Figure 2d shows that PU resin did not only covered the surface of BC, but also penetrated through the plate-like structures of BC. As a result, the air interstices of neat BC were filled with PU resin, which in turn yielded a sheet arranged by tightly compacted layers of BC nanofibers.[26]

The process of solvent exchange (i.e. water was replaced by ethyl glycol acetate) employed in the never-dried BC membranes had a notable role on the fabrication of composites with a very consistent layered structure. We believe that use of ethyl glycol acetate greatly allowed the penetration of the PU prepolymer in BC membrane because it was the common solvent in BC and PU prepolymer. The same behavior was observed by Bismark et al.[33] when never dried BC membranes were subjected to solvent exchange using only ethanol. Hopefully, the present work may contribute meaningful information on the improvement of the penetration of PU prepolymer into BC membranes by simple solvent exchange approach. The impregnation of PU resin through the BC membrane leads to new urethane bonds as highlighted by the schematic illustration pictured in Figure 3. The urethane bonds produce a strong interface between cellulose nanofibers and PU of the composite that interconnect the entire 3D network of BC nanofibers.

Once the network of BC nanofibers were not detected in the SEM of the surface of BC/PU composites, it is expected that their surface could accomplish a reduced roughness compared with the surface of pristine dried BC membrane. To confirm our hypothesis, we performed AFM analysis of the BC/PU composites and the pristine BC membrane. To date, a low

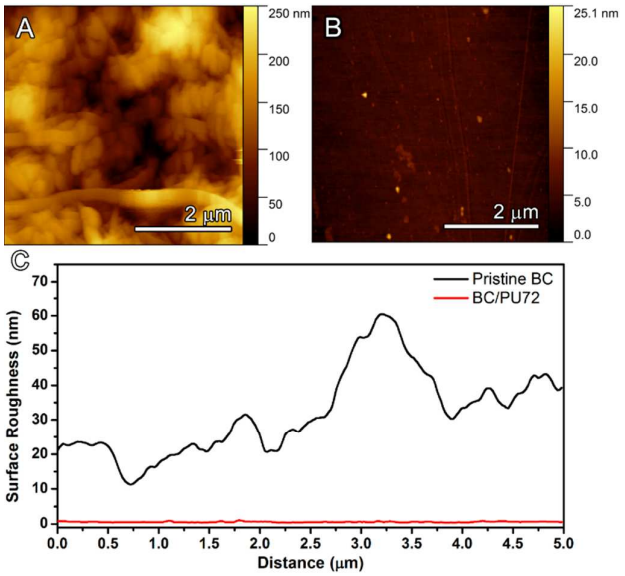

Figure 4. Top view and 3D view of AFM images from (A) pristine BC membrane and (B) BC/PU composite resulted from solvent exchange process within 72 h. (C) Graph of the surface roughness as a function of the distance for pristine BC membrane and BC/PU composite extracted from tapping mode atomic force microscopy. When the BC nanofibers were covered with PU resin, the surface roughness greatly reduced from 32 ± 12.23 nm to 0.503 ± 0.1186 nm.

surface roughness is an important requirement for substrates based on polymers and should be kept lower than 5 nm[34] for the fabrication of suitable substrates for flexible OLED. Figure 4, a and b, illustrate the top view of AFM images evaluated in contact mode for pristine BC membrane and BC/PU72 composite over an area of 25 μm^2. Figure 4c shows the plot of surface roughness (Ra) as function of the distance for pristine BC membrane and BC/PU72 composite. The Ra for pristine BC was about 32 nm and it is obviously associated to the noticeable coarse surface of 3D network of BC nanofibers. On the other hand, the Ra found for BC/PU72 composite was 0.5 nm, a value 98% lower compared to pristine BC membrane. This result confirm that the covering of BC fibrils by PU was also very effective to afford a very smooth surface. Manuspiya et al.[35] reported the fabrication of composites from BC and commercial PU resin where the surface roughness was 81.39 nm. The authors also achieved a reduced roughness of 25.66 nm by polishing the surface of the composites.[36] To the best our knowledge, our results demonstrate the smallest roughness value reported in the literature for BC/PU composites and even better than ones subjected to surface post-treatment.

Figure 5 shows the XRD patterns for pristine BC membranes, pure PU resin film, and BC/PU composites. The XRD pattern of pure PU resin film shown in Figure 5a displays a single diffuse peak at 21° in 2θ, predominantly associated with amorphous nature of the polymer. On the other hand, the nanofibers synthesized from bacteria contain a large amount of high crystalline cellulose polymer and is free of amorphous phases such as lignin and hemicellulose abundantly present in plant-derived celluloses. As a result, the dried BC membrane is basically constituted by a semi-crystalline polymer, whose XRD

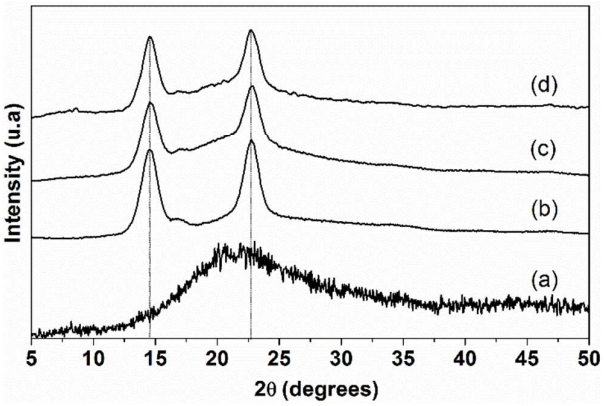

Figure 5. X- Ray diffraction of (a) pure polyurethane film; (b) Pristine dried BC membrane and BC/PU composites resulted from solvent exchange process within (c) 72 h and (d) 120 h.

pattern displays two broad reflection peaks localized at 15° and 22.5°, assigned to the 1α and 1β phases of native cellulose (i.e. type I cellulose) and overlapped by amorphous haloes.[37] The peak at 15° is related to the contribution of the reflections from the monoclinic (110) and triclinic (100) plans. The peak at 22.5° corresponds to the contribution of the reflections from the monoclinic (002) and triclinic (110).[37] Nevertheless, the BC/PU composites show similar diffraction pattern profile compared to the pristine BC membrane, suggesting that semi-crystalline structure is preserved during the experimental procedure. For clarity, we investigated the influence of the impregnation of PU in the cellulose by means of the calculus of the crystallinity of BC membranes and BC/PU composites. To this end, we applied the Segal´s equation[38] (eq. 1) into the extracted data from XRD diffraction,

$$CrI = \frac{I_{002} - I_{100}}{I_{002}} \; x \; 100 \quad \text{(eq. 1)}$$

where CrI corresponds the relative degree of crystallinity, I_{002} is the maximum intensity of the (002) plane diffraction and I_{am} is the intensity of the amorphous halo at 2θ = 18°. According to the Segal´s equation, pristine BC membrane shows CrI value equal to 70 %.[38] However, a slight decrease in crystallinity is observed after the impregnation of PU resin resulting a CrI value of 64% for all BC/PU composites. We propose that the PU resin could penetrate into the cellulose chains and promote the breakdown of inter-chains hydroxyl hydrogen bonds, thereby causing the decrease of the BC crystallinity.[39]

Thermal stability of the pure BC, PU film, and BC/PU composites was conducted by thermogravimetric analysis (not show here). Although BC/PU composite showed higher thermal stability (248 °C to BC/PU72 and 266.5 °C to

Table 2. Mechanical properties of the BC/PU composites compared to Pristine BC membranes and pure PU film

	Stress (MPa)	Strain (%)	Young's Module (GPa)
Pristine BC	179.9	2.6	13
BC/PU72	69.5	1.9	6.0
BC/PU120	65.8	2.1	4.7
Pure PU film	2.3	24.5	0.016

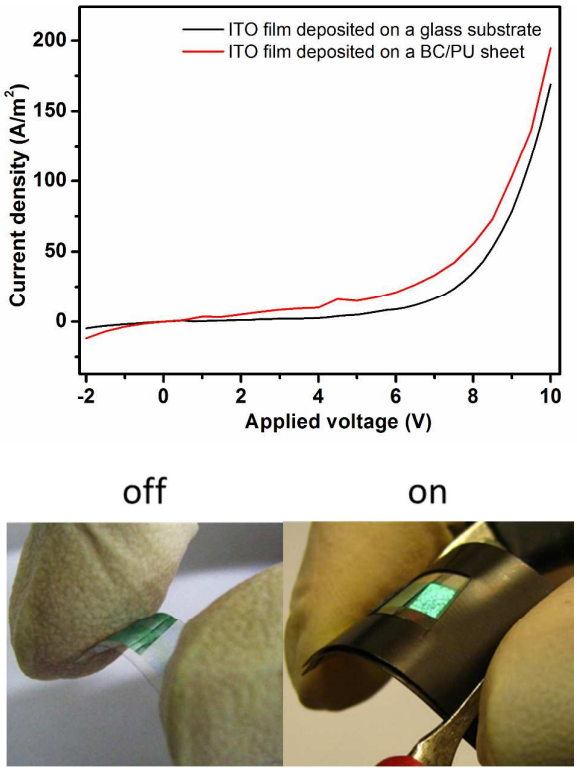

Figure 6. Plot of the current density versus applied voltage curves for BC/PU composite resulted from exchange solvent process within 72 h and flat glass substrate, both coated with an indium-tin-oxide layer. The bottom section is shown Digital images of the working flexible OLEDs onto BC/PU composite when switched from "on" and "off" state. A black paper was placed around the transparent BC/PU to highlight the greenish brightness of the deposited electroluminescent layer when the substrate is switched to the "on" state.

BC/PU120) comparing to pure PU film (233 ºC), they display a thermal stability substantially lower than pristine BC membrane (300 °C). The increase of thermal degradation temperature of BC/PU composites compared to the pure PU film could be attributed to the strong interface of PU prepolymer and BC nanofibers, generating the previously mentioned cross-linked network of obtained along the cure process with moisture air.

Besides high transparency, thermal stability and low surface roughness, a highly desired substrate for flexible OLED market, for example, should present obvious remarkable mechanical properties. Lately, word's leading glass manufacturers have unveiled a great effort to introduce glass-based flexible substrates for OLED displays and lightening. For example, Corning® have developed an ultra-thin substrate (50 µm) known as Willow glass™ commercially studied as potential alternative as substrate of flexible OLED devices. Although it shows exceptional flexibility, it has been reported that such glassy substrate exhibited shattering issues when the edges are stressed.[40] The BC/PU composites proposed in this work are thinner than the glass-based substrates and can reversibly bend into acute angles even when stressed on the edges. A more detailed investigation of the mechanical properties of BC/PU composites was conducted by Dynamic Mechanical Analysis using strips cut samples. The tensile stress at break and Young's modulus of the BC/PU composites were compared with the pristine BC membranes and pure PU film as summarized in Table 2.

Pure PU film is basically composed majority by castor oil based polyurethane polyether or polyester soft segments and by diisocyanate-based hard segments. Evidently, these features are greatly pronounced in the low tensile stress and Young's modulus of the PU pure films comparing to BC/PU composites. Additionally, the PU film displayed significant deformation with a tensile strain of 24.5 MPa. The increase of both tensile stress at break and Young's modulus were consistent with the increase of cellulose content in the composites. In fact, BC/PU composites loaded with high content of cellulose outperform enhancements with strength up to 69 MPa and Young's modulus up to 6 GPa presumably because the outstanding mechanical properties of individual BC nanofibers.

Remarkably, the facile combination of two special materials derived from renewable sources, namely castor oil based polyurethane and BC membranes, lies to flexible and transparent composites. Although transparent substrates based on cellulosic resins are abundantly reported in the literature, there are still few successful works of their applications in flexible electronics. The BC/PU composites were evaluated as compatible substrate for the fabrication of flexible OLED.

The OLED substrates were prepared by the deposition of a conductive thin film of ITO onto the surface of BC/PU membrane and glass substrate. The electrical characteristic of both samples are detailed in Table 3. As it can be seen, ITO electrical characteristics measured onto BC/PU surface were similar to that of the ITO onto glass. This result also confirms a superior result when compared with the pristine BC based flexible OLED published in previous work.[5] Despite the excellent surface roughness found in BC/PU composites, the resistivity of ITO layer is slightly larger for the composites than flat glass substrates. We conceive that the deviation of resistivity value might be attributed to the flexible feature of BC/PU substrate. Both flexible OLED and OLED presented the standard diode current density as function of the applied voltage curve, as shown in Figure 6. Furthermore, when compared with glass substrate, BC/PU flexible OLED displayed an improved electrical performance since a higher current density with lower applied voltage was achieved when compared with flat glass substrate.

We investigated the luminance of the flexible OLED and OLED for both BC/PU and glass substrates by applying the same current density and tension through the device, about 20 $A.m^{-2}$ and 10 V. The measurement was performed in triplicate and the luminance results of the flexible OLED were 231 ±18 $cd.m^{-2}$

Table 3. Electrical characterization of indium-tin-oxide thin film deposited onto the surface of a BC/PU composite resulted from exchange solvent process within 72 h and flat glass substrate.

	Carrier number ($\times 10^{20}$ cm^{-3})	Carrier mobility ($cm^2.V^{-1}.s^{-1}$)	Resistivity ($\times 10^{-4}$ Ω.cm)
BC/PU72	-5.17	20.89	5.78
Glass	-9.55	19.89	3.29

for BC/PU and 485 ± 8 cd.m^{-2} for flat glass substrate. It should be noted that technical difficulties were found when measuring luminance of flexible OLED due to the occurrence of folds during the acquisition. This might have negatively influenced on the flexible OLED luminance result. Additionally, Figure 6 shows the digital images of transparent flexible OLED built on BC/PU composites switched between on/off states.

A high quality ITO deposition was accomplished onto freestanding films of BC/PU composite. Because the high transparency (> 90 %) and flexibility, we suggest that BC/PU composites are potential candidates for substrate of flexible electronic display device.

Conclusions

Flexible and transparent freestanding films of bacterial cellulose (BC) and castor oil based polyurethane (PU) prepolymer were fabricated by an ease solvent exchange protocol. The BC/PU composites comprises thin free-standing films (< 50 μm) displaying high transparency in the ultraviolet (up to 70% at 350 nm) and visible region (i.e. up to 90 % at 700 nm) besides low surface roughness (< 1 nm) which are fundamental requisites of substrates for lighting-emitting devices and displays. Additionally, BC/PU composites were semi-crystalline and displayed good thermal stability (> 250 °C). In fact, the introduction of polyurethane endows exceptional improvement on the optical properties of BC membranes while the addition of BC nanofibers delivers the fabrication of films with higher breaking strength. The accomplishment of flexible and transparent composites is due to the unique interface between BC nanofiber surface and PU prepolymer. It is important to note that the uniformity of distribution of PU throughout the 3D network of BC nanofibers was remarkably achieved only via exchange solvent process rather than other methods (e.g. hot pressed and UV-curing methods) used in the literature. The BC/PU composites features offer exciting new opportunities as substrate for flexible electronic displays. Besides, it must be considered that bacterial cellulose and castor oil are obtained from renewable resources and can potentially be subjected to conventional decomposition by microorganisms in soil, along with the degraded production of H_2O, CO_2, and aromatic ethers.

Acknowledgements

Financial support from Brazilian agencies: State of São Paulo Research Foundation (FAPESP), Coordination for the Improvement of Higher Education Personnel (CAPES) and National Council for Scientific and Technological Development (CNPq) and technical support of Electron Microscopy Laboratory (LME, Araraquara, BR) are acknowledged.

Notes

‡ These authors contributed equally to this work.

References

1. D. Klemm, F. Kramer, S. Moritz, T. Lindstrom, M. Ankerfors, D. Gray and A. Dorris, *Angewandte Chemie*, 2011, **50**, 5438-5466.
2. G. Guhados, W. Wan and J. L. Hutter, *Langmuir*, 2005, **21**, 6642-6646.
3. A. Nakagaito and H. Takagi, in *Handbook of Polymer Nanocomposites. Processing, Performance and Application*, eds. J. K. Pandey, H. Takagi, A. N. Nakagaito and H.-J. Kim, Springer Berlin Heidelberg, 2015, ch. 68, pp. 343-353.
4. B. Geffroy, P. Le Roy and C. Prat, *Polymer International*, 2006, **55**, 572-582.
5. C. Legnani, C. Vilani, V. L. Calil, H. S. Barud, W. G. Quirino, C. A. Achete, S. J. L. Ribeiro and M. Cremona, *Thin Solid Films*, 2008, **517**, 1016-1020.
6. M. D. J. Auch, O. K. Soo, G. Ewald and C. Soo-Jin, *Thin Solid Films*, 2002, **417**, 47-50.
7. Y. Okahisa, A. Yoshida, S. Miyaguchi and H. Yano, *Composites Science and Technology*, 2009, **69**, 1958-1961.
8. T. Nishino, I. Matsuda and K. Hirao, *Macromolecules*, 2004, **37**, 7683-7687
9. M. Nogi and H. Yano, *Advanced Materials*, 2008, **20**, 1849 - 1852.
10. S. C. M. Fernandes, L. Oliveira, C. S. R. Freire, A. J. D. Silvestre, C. Pascoal Neto, A. Gandini and J. Desbrieres, *Green Chemistry*, 2009, **11**, 2023-2029.
11. H. S. Barud, J. L. Souza, D. B. Santos, M. S. Crespi, C. A. Ribeiro, Y. Messaddeq and S. J. L. Ribeiro, *Carbohydrate Polymers*, 2011, **83**, 1279-1284.
12. C. Tang and H. Liu, *Composites Part A: Applied Science and Manufacturing*, 2008, **39**, 1638-1643.
13. H. S. Barud, J. M. A. Caiut, J. Dexpert-Ghys, Y. Messaddeq and S. J. L. Ribeiro, *Composites Part A: Applied Science and Manufacturing*, 2012, **43**, 973-977.
14. Y. Kim, R. Jung, H. S. Kim and H. J. Jin, *Current Applied Physics*, 2009, **9**, S69-S71.
15. H. Yano, J. Sugiyama, A. N. Nakagaito, M. Nogi, T. Matsuura, M. Hikita and K. Handa, *Advanced Materials*, 2005, **17**, 153 - 155.
16. C. K. Williams and M. A. Hillmyer, *Polymer Reviews*, 2008, **48**, 1-10.
17. A. Zlatanić, C. Lava, W. Zhang, Z. S. Petrović, *Journal of Polymer Science Part B: Polymer Physics*, 2004, **42**, 809-819.
18. V. D. Athawale and P. S. Pillay, *Journal of Polymer Materials*, 2003, **20**, 317-326.
19. H. Mutlu and M. A. R. Meier, *European Journal of Lipid Science and Technology*, 2010, **112**, 10-30.
20. H. J. Wang, M. Z. Rong, M. Q. Zhang, J. Hu, H. W. Chen and T. Czigany, *Biomacromolecules*, 2008, **9**, 615-623.
21. C. Zhang, H. Wu and M. R. Kessler, *Polymer*, 2015, **69**, 52-57.
22. V. R. Botaro, A. Gandini and M. N. Belgacem, *Journal of Thermoplastic Composite Materials*, 2005, **18**, 107-117.
23. D. Klemm, D. Schumann, F. Kramer, N. Hessler, M. Hornung, H. P. Schmauder and S. Marsch, *Polysaccharides II*, 2006, **205**, 49-96.
24. P. Chen, S. Y. Cho and H. J. Jin, *Macromolecular Research*, 2010, **18**, 309-320.
25. S. J. Eichhorn, A. Dufresne, M. Aranguren, N. E. Marcovich, J. R. Capadona, S. J. Rowan, C. Weder, W. Thielemans, M. Roman, S. Renneckar, W. Gindl, S. Veigel, J. Keckes, H. Yano, K. Abe, M. Nogi, A. N. Nakagaito, A. Mangalam, J. Simonsen, A. S. Benight, A. Bismarck, L. A. Berglund and T. Peijs, *Journal of Materials Science*, 2010, **45**, 1-33.

26. J. Juntaro, S. Ummartyotin, M. Sain and H. Manuspiya, *Carbohydrate Polymers*, 2012, **87**, 2464-2469.
27. S. Ummartyotin, J. Juntaro, M. Sain and H. Manuspiya, *Industrial Crops and Products*, 2012, **35**, 92-97.
28. K. D. Vorlop, A. Muscat and J. Beyersdorf, *Biotechnology Techniques*, 1992, **6**, 483-488.
29. I. M. Arcana, B. Bundjali, M. Hasan, K. Hariyawati, H. Mariani, S. D. Anggraini and A. Ardana, *Journal of Polymers and the Environment*, 2010, **18**, 188-195.
30. E. De Carlo, Dissertation, University of São Paulo, 2002.
31. J. Ganster and H.-P. Fink, in *Handbook of Polymers*, eds. J. Brandrup, E. H. Immergut and E. A. Grulke, John Wiley & Sons, New York, 4th edn., 1999, ch. V, pp. 135-152.
32. A. N. Nakagaito, M. Nogi and H. Yano, *MRS Bulletin*, 2010, **35**, 214-218.
33. J. Juntaro, M. Pommet, A. Mantalaris, M. Shaffer and A. Bismarck, *Composite Interfaces*, 2007, **14**, 753-762.
34. M.-C. Choi, Y. Kim and C.-S. Ha, *Progress in Polymer Science*, 2008, **33**, 581-630.
35. S. Ummartyotin, J. Juntaro, M. Sain and H. Manuspiya, *Carbohydrate Polymers*, 2011, **86**, 337-342.
36. S. Ummartyotin, J. Juntaro, M. Sain and H. Manuspiya, *Chemical Engineering Journal*, 2012, **193**, 16-20.
37. M. Wada, J. Sugiyama and T. Okano, *Journal of Applied Polymer Science*, 1993, **49**, 1491-1496.
38. L. Segal, J. J. Creely, A. E. Jr Martin and C. M. Conrad, *Textile Research Journal*, 1959, **29**, 786-794.
39. D. T. B. De Salvi, H. S. Barud, J. M. A. Caiut, Y. Messaddeq and S. J. L. Ribeiro, *Journal of Sol-Gel Science and Technology*, 2012, **63**, 211-218.
40. G. Mone, *Communications of the ACM*, 2013, **56**, 16-17.

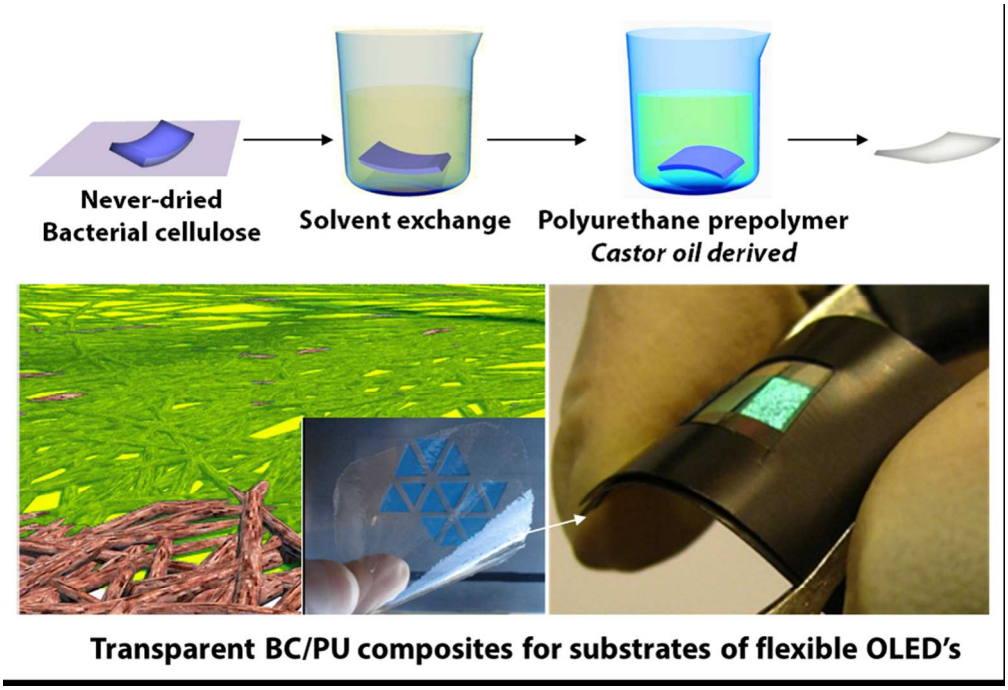

181x123mm (150 x 150 DPI)